ASHA American Speech-Language-Hearing Association

JSLHR

Research Note

An Exploratory Investigation of the Palatoglossus Muscle in Children Using Magnetic Resonance Imaging

Samantha Power[a] and **Katelyn J. Kotlarek**[a]

[a] Division of Communication Disorders, University of Wyoming, Laramie

ARTICLE INFO

Article History:
Received May 25, 2022
Revision received July 20, 2022
Accepted July 20, 2022

Editor-in-Chief: Cara E. Stepp
Editor: Kate Bunton

https://doi.org/10.1044/2022_JSLHR-22-00303

ABSTRACT

Purpose: There is currently little evidence reporting the typical morphology of the palatoglossus (PG) muscle. The primary purpose of this exploratory study is to determine whether magnetic resonance imaging (MRI) methods used to quantify the morphology of the levator veli palatini (LVP) muscle can be applied to the PG. The secondary purpose is to provide preliminary data regarding the relationship between the LVP and PG muscles in children.
Method: Ten children between ages of 4 and 7 years participated in this study. Each participant was scanned using a nonsedated, child-friendly protocol with a T2-weighted, three-dimensional anatomical scan to obtain images of the oropharyngeal anatomy. Custom, oblique-coronal image planes were created to visualize and measure the LVP and PG muscles in their entirety from origin to insertion. Thermo Scientific Amira Software was used to obtain 2D measurements of PG muscle length, width, velar insertion distance, lingual insertion distance, and several angle measurements.
Results: The PG ranged from 17.95 to 26.96 mm in length across participants. Velar insertion distance ranged from 17.22 to 30.95 mm. Lingual insertion distance ranged from 26.91 to 36.02 mm. Width ranged from 2.32 to 3.08 mm. The angle formed by the PG and LVP muscle planes ranged from 7.3° to 52.7°. The LVP insertion angle ranged from 42.5° to 75.9°. The PG insertion angle ranged from 16.9° to 52.3°.
Conclusions: MRI was successful in visualizing the PG muscle. The PG was consistent in size and shape within an individual participant but varied across the participant cohort.

The palatoglossus (PG) muscle is categorized as both an extrinsic muscle of the tongue and a muscle of the velopharyngeal mechanism. The PG originates from the palatine aponeurosis, which is located on the oral surface of the palate stretching from the crest of the palatine bone of the hard palate through the first two thirds of the soft palate. The PG courses laterally, inferiorly, and anteriorly from the palatine aponeurosis creating the arch of the anterior faucial pillars and inserts into the sides of the posterior two thirds of the tongue (Du Brul, 1976; Woodburn, 1973). Du Brul (1976) hypothesized that the PG continues toward the midline of the tongue, intermingling with transverse muscles of the tongue and creating a sphincter with the surrounding intrinsic muscle fibers. The anatomical positioning of the PG implies that the muscle could have multiple functions during velar and lingual movements for both swallowing and speech production.

Researchers have consistently agreed that the movements of the PG assist in early stages of deglutition (Goldie et al., 2006; Lubker et al., 1970; Lubker & May, 1973; Perry, 2011). The contraction of the PG elevates the base of the tongue and constricts the oropharyngeal isthmus by pulling the anterior faucial pillars medially toward the tongue (Du Brul, 1976; Fritzell, 1969; Gick et al., 2014; Perry, 2011). There is a lack of agreement on the role of the PG in connected speech, specifically velar lowering and positioning. Studies have found the PG to exert

Correspondence to Katelyn J. Kotlarek: kkotlare@uwyo.ecu. ***Disclosure:*** *The authors have declared that no competing financial or nonfinancial interests existed at the time of publication.*

force on the inferior third of the velum, making it the direct antagonist of the levator veli palatini (LVP; Berry et al., 1999; Kuehn et al., 1982; Perry, 2011). Some have suggested that the PG lowers the velum specifically for nasal sounds (Dixit et al., 1987; Fritzell, 1969; Lubker et al., 1970; Perry, 2011). Others have found evidence of the PG being actively involved in the overall velar positioning of central, back, and low vowels in addition to nasal phonemes (Berry et al., 1999; Dixit et al., 1987). Further findings validated the presence of a temporal relationship between PG and LVP muscle activation for overall velar positioning (Kuehn et al., 1982). In summary, the literature supports that the PG is involved in elevation of the tongue base and most likely has some role in velar lowering and overall velar positioning.

While our understanding of the function of the PG is evolving, there is still little known about the typical morphology of this muscle. Most of our anatomical knowledge regarding the PG comes from cadaveric studies, both gross dissection and histological. Kuehn and Azzam (1978) utilized gross dissection of cadavers to first quantify the muscle shape at its widest diameter and hypothesize force vectors for muscle action. Great variability in the PG force vector was observed across participants resulting from variations in typical morphology and reinforcing the need for further research in this area (Kuehn & Azzam, 1978). Additional research has focused largely on muscle activity during speech rather than morphology (Bell-Berti, 1976; Benguerel et al., 1977; Kuehn, 1980; Kuehn et al., 1982; Lubker et al., 1970; Lubker & May, 1973; Moon et al., 1994; Smith & Hirano, 1968). From previous literature, it is difficult to grasp the full nature of the PG from the origin to insertion since no studies have directly visualized the PG muscle in living individuals, including children.

Several studies have employed magnetic resonance imaging (MRI) to visualize other velopharyngeal muscles in vivo to obtain normative data on size and shape. MRI is the only imaging modality that allows for visualization of the velopharyngeal musculature in living individuals. Ettema et al. (2002) were the first to use MRI to quantify LVP morphology. The resulting data set was the first of its kind and demonstrated successful use of two-dimensional (2D) MRI to measure a primary muscle of the velopharyngeal mechanism. Since this foundational study, improved MRI protocols utilizing three-dimensional (3D) imaging technology have become the gold standard for visualizing and analyzing velopharyngeal anatomy. The LVP has been the primary velopharyngeal muscle of focus across the lifespan, with several studies analyzing the normative structure of this muscle in younger participants such as children (Kollara & Perry, 2014; Kollara et al., 2016; Perry et al., 2018) and infants (Kotlarek, Levene, et al., 2022; Schenck et al., 2016). The morphology of the musculus uvulae, salpingopharyngeus, and tensor veli palatini has been analyzed using similar MRI protocols (George et al., 2018; Perry et al., 2019; Perta et al., 2021). Such investigations have led to a robust knowledge base regarding typical and atypical velopharyngeal anatomy.

To the best of our knowledge, there are no studies reporting measures of the PG muscle in children. A further understanding of PG morphology may provide insight into the muscle's function for normal and abnormal tongue and velopharyngeal control. As a muscle of the velopharynx and the direct antagonist to the LVP, variations in PG morphology may adversely impact velopharyngeal function; as an extrinsic muscle of the tongue, PG variations may also impact positioning of the tongue dorsum. Thus, the purpose of this exploratory study is to determine if MRI methods previously used to study other velopharyngeal muscles can be applied to the PG muscle to yield quantitative data regarding PG morphology. The secondary purpose is to provide preliminary data regarding the relationship between the LVP and PG muscles in children. Based on previous research, it was hypothesized MRI would prove to be successful in visualizing the PG muscle. Additionally, it was hypothesized that the PG would be consistent in shape across participants but the orientation of the PG relative to the LVP would vary.

Method

Participants

This study was approved by the East Carolina University Institutional Review Board, and an Institutional Affiliation Agreement is in place with the University of Wyoming. MRI data of 10 Caucasian children between the ages of 4 and 7 years were selected from a pre-existing database. Other participant demographics are reported in Table 2. All participants were free of craniofacial or musculoskeletal anomalies and displayed typical resonance as evaluated by a speech-language pathologist with 5 years of experience assessing resonance disorders.

MRI Protocol

Two scanners were used in this study due to geographical distance within the recruitment area. Both scanners were 1.5 Tesla Siemens magnets, and consistent imaging protocols were used between both locations. Participants were imaged in the supine position while the velum rested on the tongue base. None of the participants were sedated during imaging. Participant movement was minimized using cushions around each participant's head to fit snugly in the head coil. Each high-resolution, volumetric image sequence used in this study was acquired using a T2-weighted, 3D anatomical scan called SPACE

(Sampling Perfection with Application optimized Contrasts using different flip angle Evolution). The scan was localized to the nose tip to optimize the view of the oropharyngeal anatomy with at least 0.8-mm isotropic resolution. The completion time for this scan was just under 5 min.

Image Processing and Analysis

Images were uploaded and analyzed using Thermo Scientific Amira Software (Thermo Fisher Scientific). This program has a built-in native Digital Imaging and Communication in Medicine support program, which means the images can be transferred into the software and maintain proper anatomical ratios and resolution needed for accurate measures. Two custom, oblique-coronal planes coursing through the belly of both the PG and LVP muscle bundles respectively were created by hand for each participant.

Following the successful completion of a velopharyngeal MRI analysis training protocol consisting of training videos and active measuring, a single rater measured all 10 participants. 2D measurements of the PG length and width were obtained from the central-most image of the PG plane. Width was measured as the left-to-right diameter of the muscle halfway between the velar insertion and lingual insertion, perpendicular to the length of the muscle at that point. Length measurements were taken from the velar insertion to the lingual insertion of the PG using a curvilinear line to follow the natural curvature of the muscle belly. The PG–LVP angle was defined as an interior angle created by the intersection of the PG and LVP planes when overlaid on the midsagittal view. The angle is visualized as the angular space between the PG and LVP plane boundaries. To measure the PG–LVP angle, the two custom planes were overlaid on the midsagittal image. The PG–LVP angle was created and measured using the following three points: a point along the PG plane, the point of intersection of the PG and LVP planes, and a point along the LVP plane. The PG and LVP angles were also taken in reference to the spinal column. Both the PG and LVP angles were defined as interior angles as well. The angle is the space between the respective PG or LVP plane and a guideline running along the third and fourth cervical vertebrae. To measure the PG angle, the plane was overlaid on the midsagittal image. A reference line was then situated along the anterior aspect of the third and fourth cervical vertebrae. The PG angle was measured using the following three points: a point along the PG plane, the point of intersection of the PG plane and reference line, and a point along the reference line. The same was done using the LVP plane. All measurements are defined in Table 1. Measurements are shown in Figure 1.

Statistical Treatment

Descriptive statistics were used to characterize the data due to the exploratory nature of this work and low sample size. A Pearson product-moment correlation was used to assess inter- and intrarater reliability. Interrater reliability was calculated using measurements taken by two researchers with experience in MRI data analysis using the measure of the LVP angle on 50% of participants (r = .905). Intrarater reliability was calculated using the LVP angle, PG angle, and PG width on all participants 1 week later, which ranged from r = .955 to .981.

Results

Quantitative Data

Measurements of the PG included length (velar insertion to lingual insertion), velar insertion distance, lingual insertion distance, muscle width, PG angle, LVP angle, and the PG–LVP angle. The PG length ranged from 17.95 to 26.96 mm (M = 21.21 mm, SD = 3.1 mm)

Table 1. Measurements and corresponding definitions.

Variable	Definition
Velar insertion distance	Linear distance from the PG velar insertion on the left side to the velar insertion on the right side
Lingual insertion distance	Linear distance from the PG lingual insertion on the left side to the velar insertion on the right side
PG length	Linear distance from the point of velar insertion to the lingual insertion
PG width	Linear, side-to-side diameter of the muscle halfway between the velum and tongue
LVP (sagittal) angle	Interior angle created by the intersection of the oblique coronal plane of the LVP muscle and a guideline running along the anterior aspect of the third and fourth cervical vertebrae from the midsagittal view
PG angle	Interior angle created by the intersection of the oblique coronal plane of the PG muscle and a guideline running along the anterior aspect of the third and fourth cervical vertebrae from the midsagittal view
PG–LVP angle	Interior angle created by the intersection of the oblique coronal plane of the PG muscle and the oblique coronal plane of the LVP muscle from the midsagittal view

Note. PG = palatoglossus; LVP = levator veli palatini.

Figure 1. The midsagittal image (left) showing the palatoglossus (PG) angle (red), the levator veli palatini (LVP) angle (green), and PG–LVP angle (blue). An oblique coronal image (right), showing PG length, PG width, velar insertion distance, and lingual insertion distance.

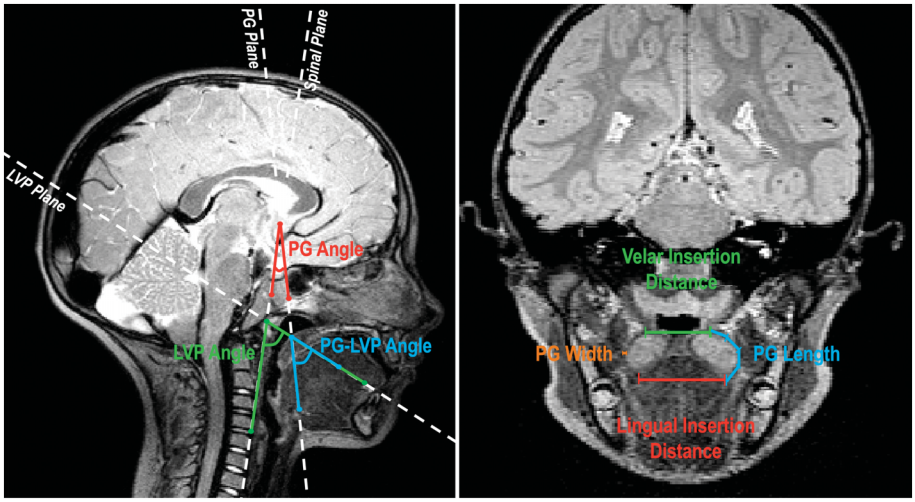

across participants. Velar insertion distance is the distance measured from the velar insertion on the right side to the velar insertion on the left side; velar insertion distance ranged from 17.22 to 30.95 mm (M = 26.62 mm, SD = 3.9 mm). Lingual insertion distance is the distance measured from the lingual insertion of the PG on the right side to the lingual insertion on the left side; lingual insertion distance ranged from 26.91 to 36.02 mm (M = 31.80 mm, SD = 2.5 mm). In addition, PG width was measured at the midpoint directly between the velar insertion and lingual insertion, where the muscle belly appeared to be flattened within the anterior faucial pillar; the measurements ranged from 2.32 to 3.08 mm (M = 2.79 mm, SD = 0.24 mm). The angle measurements taken included the PG angle, LVP angle, and PG–LVP angle. The PG–LVP angle ranged from 7.3° to 52.7° (M = 30.17°, SD = 15.0°) across participants. The LVP angle ranged from 42.5° to 75.9° (M = 65.28°, SD = 11.6°). The PG angle ranged from 16.9° to 52.3° (M = 36.11°, SD = 13.8°). All measurements for all participants are listed in Table 2 along with mean and standard deviation for each measure.

Qualitative Anatomical Description

Inconsistencies in the location of the PG were observed in this study, which resulted in great variability in

Table 2. Dimensions of the palatoglossus muscle across all participants.

Demographics				Measurements						
Age	Sex	Weight	Height	Length	Width	Velar insertion distance	Lingual insertion distance	PG–LVP angle	PG angle	LVP angle[a]
4.4	M	35.9	40.0	20.58	2.32	17.22	33.53	48.7	28.5	75.9
5.0	F	40.8	42.0	18.82	2.56	26.71	31.39	37.6	37.5	74.1
5.6	F	39.8	44.0	18.73	2.84	30.15	29.98	21.6	49.9	70.7
5.7	F	41.1	46.0	17.95	2.65	28.63	32.29	22.8	48.9	71.1
5.9	M	56.0	46.5	23.28	2.98	25.43	30.5	52.7	17.2	72.2
6.7	M	48.1	48.0	24.55	3.08	28.27	33.34	44.3	22.7	63.7
6.7	M	49.0	49.0	26.96	2.72	27.32	31.0	26.3	16.9	42.5
7.3	M	49.0	51.0	18.56	3.04	30.95	33.05	7.3	41.4	46.0
7.7	F	n.d.	n.d.	20.08	2.74	27.49	26.91	15.5	52.3	66.5
7.7	M	52.5	54.0	23.58	2.97	24.02	36.02	24.9	45.8	70.1
Mean (*SD*)		46.55[b] (6.7)	46.72[b] (4.4)	21.21 (3.1)	2.79 (0.24)	26.62 (3.9)	31.80 (2.5)	30.17 (15.0)	36.11 (13.8)	65.28 (11.6)

Note. All measurements are in millimeters (mm) with the exception of angle measures (°), age (y), weight (lbs), and height (in). PG = palatoglossus; LVP = levator veli palatini; M = male; F = female; n.d. = missing data.

[a]LVP angle has been reported as sagittal angle in previous literature [b]Mean and standard deviation of weight and height are based on nine participants.

the PG angle and PG–LVP angle across participants. The LVP angle was fairly consistent (ranging between 42.5° and 75.9°) across participants. With the exception of two participants (42.5° and 46.0°), LVP angle measurements were within 13° of each other (range: 63.7°–75.9°). The consistency of the LVP angle can be attributed to the consistent location of the LVP plane across participants; in comparison, the PG plane and resulting angle measurement were visually more inconsistent. Figure 3 (left) displays a PG plane nearly perpendicular to the LVP plane, whereas the right image shows the PG plane running nearly parallel to the LVP plane. Variability can also be seen in the shape of the muscle across participants. Figure 2 displays the oblique-coronal images used to visualize the PG muscle. The bilateral muscle is consistent in shape within an individual. Image 2-10 clearly shows the curve of the muscle, much like a wide but defined U-shape on both the left and right sides; Image 2-6 is similar. Image 2-5, however, shows a much less defined U-shape. The left and right sides are similar in shape but not similar to the PG muscles observed in Images 2-6 and 2-10. The bilateral PG muscle shows consistent shape and length within an individual, but variability in shape, length, and plane location is present across participants.

Discussion

Although there is a substantial literature base regarding other velopharyngeal musculature, little has previously been reported on the PG muscle's morphology. This may be due to the limitations associated with prior analysis methods (e.g., gross dissection). Using nonsedated MRI in children aged 4–7 years, our findings quantified width, length, and insertion distance (lingual and velar) as well as capturing variations in orientation. These findings serve to improve our understanding of the velopharyngeal mechanism by moving toward a more complex understanding of the anatomy and physiology of all muscles involved.

The 3D MRI protocol utilized in this study was successful in visualizing the PG. MRI has been utilized to study the velopharynx for several decades, and nonsedated protocols have more recently been applied to children. The use of MRI and the specific imaging and analysis protocols outlined by Perry et al. (2013) were successful for measuring the PG. MRI permitted a clear visualization of the majority of the PG muscle through the creation of a custom oblique-coronal plane. These findings are in accordance with not only the many investigations of the LVP muscle but also more recent applications to studying the tensor veli palatini, musculus uvulae, and salpingopharyngeus muscles (George et al., 2018; Perry et al., 2019; Perta et al., 2021). Limitations existed in the ability to track the PG muscle fibers into the velum and tongue. PG muscle fibers were undistinguishable from other velar and lingual muscle fibers upon insertion into the velum and tongue dorsum, respectively.

Length and width of the PG were relatively consistent in this study. The mean length of the PG muscle, as

Figure 2. An oblique coronal image coursing through the belly of the palatoglossus muscle for all participants. M = male; F = female; y = years.

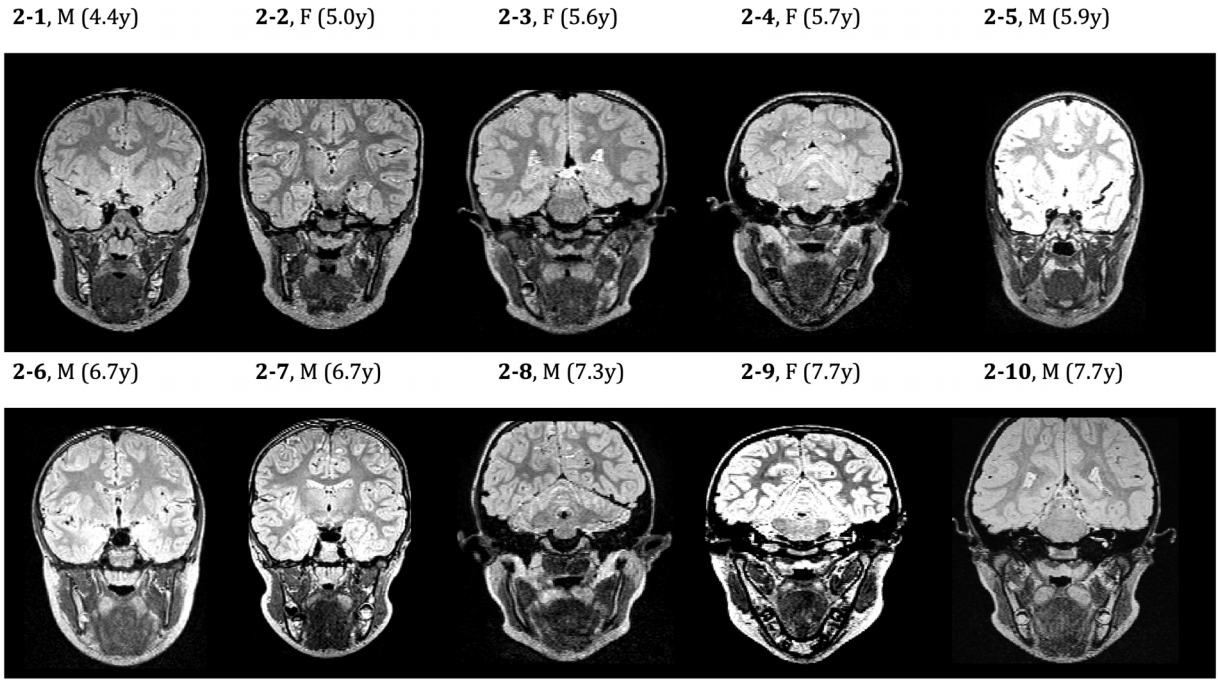

measured from the point of velar insertion to the point of lingual insertion, was 21.21 mm. The length of the PG in adults was first reported in 1910 by Hoeve. PG length was measured as the distance from the PG origin at the palatine aponeurosis to the PG insertion at the lateral edge of the tongue dorsum (Hoeve, 1910). In 1978, Kuehn and Azzam demonstrated that the PG has a fan-shaped insertion into the velum, a flattened belly within the anterior faucial pillar, and a tapered insertion into the tongue. A caliper was used to measure the widest diameter of the muscle midway between the velum and tongue; the mean diameter was 4.53 mm on the left and 3.97 mm on the right. The results of this study found the mean PG width to be 2.79 mm, which is less than findings reported by Kuehn and Azzam (1978). Based on the known impact of growth on the velopharynx, it is likely that differences in age accounted for the decreased width observed in this study. It is currently unknown how the PG changes due to growth and development, which is an important area for future study.

The LVP angle (sagittal angle) was measured and reported as a means to compare PG and LVP orientation. In 2018, Perry et al. conducted a study investigating the age, sex, and race-related differences in velopharyngeal morphology in 85 children 4–9 years of age. Perry et al. (2018) reported on several velopharyngeal variables, including the sagittal angle. Sagittal angle was significantly impacted by age, with average measurements ranging from 44.1° to 67.5° in this sample of children; specifically, the sagittal angle decreased as age increased (Perry et al., 2018). In this study, a larger LVP angle (sagittal angle) range (42.5°–75.9°) and mean (65.28°) were found. The variation in this measure between studies is likely an artifact of the small sample size employed in this study combined with the significant growth occurring at this time.

This study also identified and measured the PG–LVP interior angle by measuring the angle created by the intersection of the PG and LVP muscle planes as viewed from the midsagittal plane. The PG–LVP angle was found to be extremely variable across participants (M = 30.17°, SD = 15.0°). Based on qualitative differences observed between participants, this variability was specifically impacted by the PG angle (M = 36.11, SD = 13.8°), which did not appear to suggest any trends based on age or sex of participants. This variability between participants (despite similar LVP angles) is visually apparent in Figure 3. Kuehn and Azzam (1978) reported that the PG displayed varying force vectors across participants due to its varied positioning. Six of the nine cadavers displayed a PG force vector directed posteriorly toward the uvula, whereas the other three displayed a PG force vector directed at the opposing LVP (Kuehn & Azzam, 1978). In line with these findings, our study suggests that the location of PG attachment may present with wide variability among children as well despite differences in age. Variations in PG orientation (relative to LVP orientation) may account for observed variations in PG muscle activity during speech tasks. Future research should investigate differences in PG orientation relative to its physiology.

An understanding of the shape and orientation of typical velopharyngeal musculature in children has allowed further investigations comparing typical and atypical anatomy. Prior investigations have compared the LVP muscle morphology in children with and without cleft palate (Kotlarek et al., 2018, 2020; Kotalerk, Jaskolka, et al., 2022), submucous cleft palate (Schenck et al., 2021), and

Figure 3. The midsagittal image is shown for two participants with variations in the orientation of the palatoglossus (PG) muscle. The palatoglossus (PG) muscle plane is in red. The levator veli palatini (LVP) muscle plane is in green. Variations in the PG–LVP angle, primarily due to PG orientation, are visually apparent.

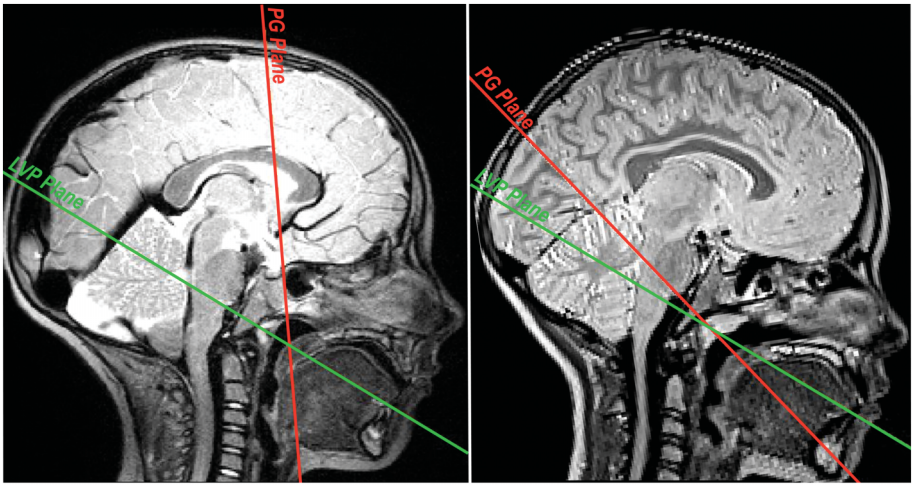

22q11.2 deletion syndrome (Kollara et al., 2019, 2021). Similar explorations have been completed in adults with cleft palate regarding other velopharyngeal muscles (George et al., 2018; Perry et al., 2019). A more robust study design is needed to draw more definitive conclusions regarding typical PG morphology before it may be used for comparisons with atypical anatomy. However, it is possible that future research may seek to address the variability observed in this study regarding PG morphology and orientation by using additional measurements and provide an opportunity for future comparison to clinically relevant populations, such as those with airway issues due to glossoptosis, Pierre Robin sequence, or Down syndrome.

Limitations

This study was limited by a small sample size. Additionally, participants ranged in age from 4.4 to 7.7 years, during which time a substantial amount of growth and development occurs in the velopharyngeal region (Perry et al., 2018, 2019). Future research should be completed using a larger sample size with multiple participants at each age to control for the impact of growth on the PG muscle and surrounding velopharyngeal anatomy. Similarly, sex and race effects on the PG muscle may be determined with a larger, more diverse sample. Prepubertal sex and race effects have previously been observed in the velopharyngeal region (Kollara et al., 2016; Kotlarek, Levene, et al., 2022; Perry et al., 2018).

Although this study demonstrated a number of novel findings, PG muscle fibers were unable to be distinguished within the palate and tongue with the use of MRI. Future use of diffusion tensor imaging (DTI) may allow for a more detailed analysis. DTI uses diffusion rates of water molecules to differentiate between tissues and allow for more specific imaging (Ranzenberger & Snyder, 2020). This may allow future research to analyze and report velopharyngeal muscle morphology in more detail and with greater precision. Completing 3D analysis of the PG muscle and integrating this information with quantitative data on surrounding structures will improve our understanding of the speech mechanism in individuals with typical and atypical anatomy.

Conclusions

MRI can be used to analyze the PG muscle in vivo. While PG width was consistent across participants, variability in the length and orientation of the PG exists across participants in childhood. Inconsistencies in the orientation of the PG resulted in a varied positional relationship between the PG and LVP across participants. Further research is needed to investigate the PG within this age range using a larger sample size to grasp a better understanding of growth, race, and sex effects on PG morphology.

Data Availability Statement

All data are included in Table 2.

Acknowledgments

Research reported in this publication was supported by the National Institute of Dental and Craniofacial Research under Award Number F31DE027878, the National Institute of General Medical Sciences under Award Number P20GM103432, the Oral Maxillofacial Surgery Foundation under a research support grant, and the University of Wyoming Honors College. Its contents are solely the responsibility of the authors and do not necessarily represent the official views of the National Institutes of Health, the Oral Maxillofacial Surgery Foundation, or the University of Wyoming. The authors would like to thank Jamie Perry, PhD, for her role in securing funding for the data set analyzed in this work.

References

Bell-Berti, F. (1976). An electromyographic study of velopharyngeal function in speech. *Journal of Speech and Hearing Research, 19*(2), 225–240. https://doi.org/10.1044/jshr.1902.225

Benguerel, A. P., Hirose, H., Sawashima, M., & Ushijima, T. (1977). Velar coarticulation in French: An electromyographic study. *Journal of Phonetics, 5,* 159–167. https://doi.org/10.1016/S0095-4470(19)31126-X

Berry, D. A., Moon, J. B., & Kuehn, D. P. (1999). A finite element model of the soft palate. *The Cleft Palate-Craniofacial Journal, 36*(3), 217–223. https://doi.org/10.1597/1545-1569_1999_036_0217_afemot_2.3.co_2

Dixit, R. P., Bell-Berti, F., & Harris, K. S. (1987). Palatoglossus activity during oral/nasal vowels of Hindi. *The Journal of the Acoustical Society of America, 79*(S1), S37–S37. https://doi.org/10.1121/1.2023199

Du Brul, E. L. (1976). Biomechanics of speech sounds. *Annals of the New York Academy of Sciences, 280*(1 Origins and E), 631–642. https://doi.org/10.1111/j.1749-6632.1976.tb25525.x

Ettema, S. L., Kuehn, D. P., Perlman, A. L., & Alperin, N. (2002). Magnetic resonance imaging of the levator veli palatini muscle during speech. *The Cleft Palate-Craniofacial Journal, 39*(2), 130–144. https://doi.org/10.1597/1545-1569_2002_039_0130_mriotl_2.0.co_2

Fritzell, B. (1969). The velopharyngeal muscles in speech: An electromyographic and cineradiographic study. *Acta Otorhinolarygologica, 250,* 1–78.

George, T. N., Kotlarek, K. J., Kuehn, D. P., Sutton, B. P., & Perry, J. L. (2018). Differences in the tensor veli palatini

between adults with and without cleft palate using high-resolution 3-dimensional magnetic resonance imaging. *The Cleft Palate-Craniofacial Journal, 55*(5), 697–705. https://doi.org/10.1177/1055665617752802

Gick, B., Anderson, P., Chen, H., Chiu, C., Kwon, H. B., Stavness, I., Tsou, L., & Fels, S. (2014). Speech function of the oropharyngeal isthmus: A modeling study. *Computer Methods in Biomechanics and Biomedical Engineering: Imaging & Visualization, 2*(4), 217–222. https://doi.org/10.1080/21681163.2013.851627

Goldie, S. J., Soutar, D. S., & Shaw-Dunn, J. (2006). The effect of surgical resection in the region of the retromolar trigone. *Journal of Plastic, Reconstructive & Aesthetic Surgery, 59*(12), 1263–1268. https://doi.org/10.1016/j.bjps.2006.05.024

Hoeve, H. J. H. (1910). *A manual of dissection and practical anatomy of head and neck*. Geo. A. Miller.

Kollara, L., Baylis, A. L., Kirschner, R. E., Bates, D. G., Smith, M., Fang, X., & Perry, J. L. (2019). Velopharyngeal structural and muscle variations in children with 22q11.2 deletion syndrome: An unsedated MRI study. *The Cleft Palate-Craniofacial Journal, 56*(9), 1139–1148. https://doi.org/10.1177/1055665619851660

Kollara, L., Baylis, A. L., Kirschner, R. E., Bates, D. G., Smith, M., Fang, X., & Perry, J. L. (2021). Interaction of the craniofacial complex and velopharyngeal musculature on speech resonance in children with 22q11.2 deletion syndrome: An MRI analysis. *Journal of Plastic, Reconstructive & Aesthetic Surgery, 74*(1), 174–182. https://doi.org/10.1016/j.bjps.2020.08.005

Kollara, L., & Perry, J. L. (2014). Effects of gravity on the velopharyngeal structures in children using upright magnetic resonance imaging. *The Cleft Palate-Craniofacial Journal, 51*(6), 669–676. https://doi.org/10.1597/13-107

Kollara, L., Perry, J. L., & Hudson, S. (2016). Racial variations in velopharyngeal and craniometric morphology in children: An imaging study. *Journal of Speech, Language, and Hearing Research, 59*(1), 27–38. https://doi.org/10.1044/2015_JSLHR-S-14-0236

Kotlarek, K. J., Jaskolka, M. S., Fang, X., Ellis, C., Blemker, S. S., Horswell, B., Kloostra, P., & Perry, J. L. (2022). A preliminary study of anatomical changes following the use of a pedicled buccal fat pad flap during primary palatoplasty. *The Cleft Palate-Craniofacial Journal, 59*(5), 614–621. https://doi.org/10.1177/10556656211014070

Kotlarek, K. J., Kotlarek, J. R., Reitnauer, P. J., & Perry, J. L. (2018). A familial case study exploring craniofacial, velopharyngeal, and speech variations in Pierre robin sequence. *Clinical Archives of Communication Disorders, 3*(3), 236–245. https://doi.org/10.21849/cacd.2018.00360

Kotlarek, K. J., Levene, S., Piccorelli, A. V., Barhaghi, K., & Neuberger, I. (2022). Growth effects on velopharyngeal anatomy within the first 2 years of life. *Journal of Speech, Language, and Hearing Research, 65*(9), 3365–3376. https://doi.org/10.1044/2022_JSLHR-22-00186

Kotlarek, K. J., Pelland, C. M., Blemker, S. S., Jaskolka, M. S., Fang, X., & Perry, J. L. (2020). Asymmetry and positioning of the levator veli palatini muscle in children with repaired cleft palate. *Journal of Speech, Language, and Hearing Research, 63*(5), 1317–1325. https://doi.org/10.1044/2020_JSLHR-19-00240

Kotlarek, K. J., Sitzman, T. J., Williams, J. L., & Perry, J. L. (2021). Nonsedated magnetic resonance imaging for visualization of the velopharynx in the pediatric population. *The Cleft Palate-Craniofacial Journal, 0*(0), 10556656211057361. https://doi.org/10.1177/10556656211057361

Kuehn, D. P. (1980). A cineradiographic and electromyographic investigation of velar positioning in non-nasal speech. *The Cleft Palate Journal, 17*(3), 216–226.

Kuehn, D. P., & Azzam, N. A. (1978). Anatomical characteristics of palatoglossus and the anterior faucial pillar. *The Cleft Palate Journal, 15*(4), 349–359.

Kuehn, D. P., Folkins, J. W., & Cutting, C. B. (1982). Relationships between muscle activity and velar position. *The Cleft Palate Journal, 19*(1), 25–35.

Lubker, J. F., Fritzell, B., & Lindquist, J. (1970). Velopharyngeal function: An electromyographic study. In *Quarterly progress and status report speech* (Vol. 4, pp. 9–20). Royal Institute of Technology, Stockholm.

Lubker, J. F., & May, K. (1973). Palatoglossus function in normal speech production. *Papers from the Institute of Linguistics, 17,* 17–26. University of Stockholm.

Moon, J. B., Smith, A. E., Folkins, J. W., Lemke, J. H., & Gartlan, M. (1994). Coordination of velopharyngeal muscle activity during positioning of the soft palate. *The Cleft Palate-Craniofacial Journal, 31*(1), 45–55. https://doi.org/10.1597/1545-1569_1994_031_0045_covmad_2.3.co_2

Perry, J. (2011). Anatomy and physiology of the velopharyngeal mechanism. *Seminars in Speech and Language, 32*(02), 83–92. https://doi.org/10.1055/s-0031-1277712

Perry, J. L., Chen, J. Y., Kotlarek, K. J., Haenssler, A. E., Sutton, B. P., Kuehn, D. P., Sitzman, T. J., & Fang, X. (2019). Morphology of the musculus uvulae in vivo using MRI and 3D modeling among adults with normal anatomy and preliminary comparisons to cleft palate anatomy. *The Cleft Palate-Craniofacial Journal, 56*(8), 993–1000. https://doi.org/10.1177/1055665619828226

Perry, J. L., Kollara, L., Kuehn, D. P., Sutton, B. P., & Fang, X. (2018). Examining age, sex, and race characteristics of velopharyngeal structures in 4- to 9-year-old children using magnetic resonance imaging. *The Cleft Palate-Craniofacial Journal, 55*(1), 21–34. https://doi.org/10.1177/1055665617718549

Perry, J. L., Kuehn, D. P., & Sutton, B. (2013). Morphology of the levator veli palatini muscle using magnetic resonance imaging. *The Cleft Palate-Craniofacial Journal, 50*(1), 64–75. https://doi.org/10.1597/11-125

Perta, K., Kalmar, E., & Bae, K. (2021). A cadaveric and magnetic resonance imaging investigation of the salpingopharyngeus. *Journal of Speech, Language, and Hearing Research, 64*(5), 1436–1446. https://doi.org/10.1044/2021_JSLHR-20-00483

Ranzenberger, L. R., & Snyder, T. (2020). *Diffusion tensor imaging*. StatPearls Publishing.

Schenck, G. C., Perry, J. L., & Fang, X. (2016). Normative velopharyngeal data in infants: Implications for treatment of cleft palate. *Journal of Craniofacial Surgery, 27*(6), 1430–1439. https://doi.org/10.1097/SCS.0000000000002722

Schenck, G. C., Perry, J. L., O'Gara, M. M., Linde, A. M., Grasseschi, M. F., Wood, R. J., Lacey, M. S., & Fang, X. (2021). Velopharyngeal muscle morphology in children with unrepaired submucous cleft palate: An imaging study. *The Cleft Palate-Craniofacial Journal, 58*(3), 313–323. https://doi.org/10.1177/1055665620954749

Smith, T. S., & Hirano, M. (1968). Experimental investigations of the muscular control of the tongue in speech. *The Journal of the Acoustical Society of America, 44*(1), 354. https://doi.org/10.1121/1.1970197

Woodburn, R. T. (1973). *Essentials of human anatomy* (5th ed.). Oxford University Press.